




## ORIGINAL RESEARCH ARTICLE

# The AGE receptor, OST48 drives podocyte foot process effacement and basement membrane expansion (alters structural composition)

Aowen Zhuang<sup>1,2,3</sup>  | Felicia Y. T. Yap<sup>3</sup> | Danielle J. Borg<sup>1</sup>  | Domenica McCarthy<sup>1</sup> |  
Amelia Fotheringham<sup>1</sup> | Sherman Leung<sup>1</sup> | Sally A. Penfold<sup>3</sup> | Karly C. Sourris<sup>3,4</sup> |  
Melinda T. Coughlan<sup>3,4</sup> | Benjamin L. Schulz<sup>5</sup> | Josephine M. Forbes<sup>1,2</sup> 

<sup>1</sup>Glycation and Diabetes Complications, Mater Research Institute – The University of Queensland, Translational Research Institute, Woolloongabba, Qld, Australia

<sup>2</sup>Faculty of Medicine, University of Queensland, St Lucia, Qld, Australia

<sup>3</sup>Baker Heart and Diabetes Institute, Melbourne, Vic, Australia

<sup>4</sup>Department of Diabetes, Central Clinical School, Monash University, Melbourne, Vic, Australia

<sup>5</sup>School of Chemistry and Molecular Biosciences, University of Queensland, St Lucia, Qld, Australia

## Correspondence

Josephine Forbes, Program Leader, Chronic Disease, Mater Research Institute – UQ, 37 Kent Street, Woolloongabba, QLD 4102, Australia.

Email: josephine.forbes@mater.uq.edu.au

Aowen Zhuang, Research Officer, Molecular Metabolism and Ageing, Baker Heart and Diabetes Institute, 75 Commercial Rd, Melbourne, VIC 3004, Australia.

Email: aowen.zhuang@baker.edu.au

## Funding information

This work has been supported by National Health Medical Research Council (NHMRC) Australia, Juvenile Diabetes Research Foundation (JDRF), Kidney Health Australia (KHA) and the Mater Research Foundation

## Abstract

**Aims:** The accumulation of advanced glycation end products is implicated in the development and progression of diabetic kidney disease. No study has examined whether stimulating advanced glycation clearance via receptor manipulation is reno-protective in diabetes. Podocytes, which are early contributors to diabetic kidney disease and could be a target for reno-protection.

**Materials and methods:** To examine the effects of increased podocyte oligosaccharyltransferase-48 on kidney function, glomerular sclerosis, tubulointerstitial fibrosis and proteome (PXD011434), we generated a mouse with increased oligosaccharyltransferase-48kDa subunit abundance in podocytes driven by the podocin promoter.

**Results:** Despite increased urinary clearance of advanced glycation end products, we observed a decline in renal function, significant glomerular damage including glomerulosclerosis, collagen IV deposition, glomerular basement membrane thickening and foot process effacement and tubulointerstitial fibrosis. Analysis of isolated glomeruli identified enrichment in proteins associated with collagen deposition, endoplasmic reticulum stress and oxidative stress. Ultra-resolution microscopy of podocytes revealed denudation of foot processes where there was co-localization of oligosaccharyltransferase-48kDa subunit and advanced glycation end-products.

**Conclusions:** These studies indicate that increased podocyte expression of oligosaccharyltransferase-48 kDa subunit results in glomerular endoplasmic reticulum stress and a decline in kidney function.

## KEYWORDS

advanced glycation end-product receptor 1, advanced glycation end-products, diabetes, diabetic kidney disease, endoplasmic reticulum stress, oligosaccharyltransferase-48 diabetic nephropathy

Benjamin L Schulz and Josephine M Forbes contributed equally to this manuscript.

This is an open access article under the terms of the Creative Commons Attribution License, which permits use, distribution and reproduction in any medium, provided the original work is properly cited.

© 2021 The Authors. *Endocrinology, Diabetes & Metabolism* published by John Wiley & Sons Ltd.

## 1 | INTRODUCTION

There is a rising global pandemic of diabetes,<sup>1,2</sup> defined by persistent hyperglycaemia, a principal risk factor for the development of concomitant chronic complications.<sup>3,4</sup> Hence, the numbers of individuals with diabetic kidney disease (DKD), a major complication, are burgeoning. DKD is an important risk factor for both end-stage kidney disease and cardiovascular disease.<sup>3,5</sup> While renin-angiotensin system blockade including angiotensin-converting-enzyme inhibition is first-line therapy for DKD, in general these agents only achieve a ~20% reduction in end-stage kidney disease.<sup>6</sup>

Advanced glycation end products (AGEs) are a heterogeneous and complex group of non-enzymatic, post-translational modifications to amino acids and proteins, which include haemoglobin A<sub>1c</sub> (HbA<sub>1c</sub>) a clinical marker used for the diagnosis of diabetes. Their endogenous formation can be exacerbated by chronic hyperglycaemia and oxidative stress<sup>7</sup> and therefore the accumulation of AGEs occurs at an accelerated rate in diabetes.<sup>8,9</sup> Increases in AGE formation on skin collagen<sup>10-12</sup> and within the circulation<sup>13,14</sup> predict poor prognosis for patients with diabetes including increased risk for kidney and cardiovascular disease. The kidneys are a major site of AGE detoxification through the filtration of circulating AGEs and their subsequent active uptake and excretion.<sup>15,16</sup> Therefore, AGE accumulation is seen in diabetic patients with chronic kidney disease.<sup>17,18</sup> Therapies which lower AGE accumulation have shown benefit in Phase II clinical trials for the treatment DKD in individuals with Type 2 diabetes.<sup>19</sup> Other AGE lowering therapies tested in clinical trials in DKD include pimagedine<sup>20</sup> which was withdrawn due to safety concerns, alagebrium chloride (ALT-711) which reached Phase II trials that were not completed due to financial constraints and benfotiamine which has shown mixed results.<sup>21</sup>

OST48, an evolutionarily conserved type 1 transmembrane protein,<sup>22</sup> is encoded by the *DDOST* (Dolichyl-diphosphooligosaccharide–protein glycosyltransferase 48 kDa subunit) gene and has been postulated to function as a receptor for AGE turnover and clearance.<sup>23,24</sup> OST48 is expressed in most cells and tissues,<sup>25</sup> including macrophages<sup>26</sup> and mononuclear cells.<sup>27</sup> In the kidney, previous studies have shown OST48 expression in glomerular cells including podocytes<sup>25,28</sup> and mesangial cells<sup>26</sup> where in the podocytes it is postulated to mediate the uptake and secretion of AGEs.<sup>29</sup> The process whereby AGEs are cleared by OST48 in the kidney is not well understood,<sup>30</sup> but is thought to involve degradation of AGEs and then excretion via the urine.<sup>31</sup> A strong link exists between impaired podocyte function and albuminuria, increased urinary AGE excretion and glomerulosclerosis.<sup>32-37</sup>

Early damage to the glomeruli, specifically podocyte structural damage, is characteristic of DKD.<sup>38-40</sup> AGEs can induce podocyte cell-cycle arrest,<sup>41</sup> hypertrophy<sup>41</sup> and apoptosis,<sup>42</sup> while a systemic reduction in AGEs has been shown to improve podocyte and kidney function.<sup>43</sup> Hence, increased facilitation of AGE excretion by increasing OST48 expression could potentially improve podocyte

health and alleviate DKD. Currently, there are no reported studies identifying whether podocyte OST48 facilitates urinary AGE excretion and subsequently if targeting podocyte OST48 could influence kidney health.

Here, we examined if facilitating greater AGE clearance via modestly increasing podocyte-specific OST48 expression could attenuate the development and progression of DKD.

## 2 | RESULTS

### 2.1 | Generation of a podocyte-specific OST48 knock-in mouse model

Mice were generated with a podocyte-specific knock-in of human OST48 (*DDOST*<sup>+/-Pod-Cre</sup>) driven by the podocin promoter (Supplementary Information 1A-B) inserted at the ROSA26 locus and showed no differences in any anthropometric parameters or long-term glycaemic control (Table 1). We have previously confirmed that this genetic modification does not affect N-glycosylation machinery.<sup>44</sup> Mice with experimentally induced diabetes were characterized by elevated fasting blood glucose and glycated haemoglobin (GHb) (Table 1). Irrespective of genotype, diabetic mice exhibited a lower body weight, renal hypertrophy, increased consumption of food and water and a greater urinary output when compared with non-diabetic mice (Table 1).

### 2.2 | *DDOST*<sup>+/-Pod-Cre</sup> mice had podocyte-specific increases in OST48 protein content

SWATH-MS proteomics measured the relative abundance of OST48 in renal cortices (Figure 1A) and identified that *DDOST*<sup>+/-Pod-Cre</sup> mice had a significant increase in OST48 protein abundance (2.06-fold). Moreover, SWATH-MS proteomes of glomeruli (Figure 1B; left) and tubular-enriched (Figure 1B; right) fractions revealed that *DDOST*<sup>+/-Pod-Cre</sup> mice each specifically had significant increases in OST48 abundance (2.59-fold and 1.79-fold, respectively). Interestingly, it appeared that there was also a significant interactive effect of diabetes on the abundance of OST48 in glomeruli (Figure 1B; left). Localized increases in OST48 abundance in WT-1 positive cells were demonstrated in *DDOST*<sup>+/-Pod-Cre</sup> mice by confocal microscopy (Figure 1C). A podocyte-specific increase in OST48 expression was confirmed using ultra-resolution three-dimensional structured illumination microscopy (3D-SIM) (Figure 1D). This included increased localization of OST48 to damaged podocyte foot processes, as indicated by nephrin loss (Figure 1D), which was particularly evident in 3D reconstruction videos (Figure S2A and Video S1). This localization of OST48 to areas of damaged foot processes was unexpected, since the prevailing model is that increasing OST48 abundance could improve declining kidney function by sequestering AGEs.<sup>45</sup> These initial findings of damage to podocyte

TABLE 1 Anthropometric and metabolic parameters

	Treatment	wild-type	wild-type	<i>DDOST+/-<sup>Pod-Cre</sup></i>	<i>DDOST+/-<sup>Pod-Cre</sup></i>	Two-way ANOVA		
	(STZ induction)	non-diabetic	diabetic	non-diabetic	diabetic	G	D	G•D
Body weight (g)	12 weeks	32.82 ± 3.12	27.14 ± 2.48	32.00 ± 4.62	26.56 ± 4.16	0.93	<b>0.0001</b>	0.59
Kidney weight (g × body weight 10 <sup>3</sup> )	12 weeks	11.62 ± 1.44	14.74 ± 2.27	11.03 ± 1.21	15.93 ± 3.91	0.74	<b>0.0001</b>	0.33
Food consumption (g/24 h)	2 weeks	3.26 ± 0.80	3.62 ± 0.49	3.63 ± 1.12	2.70 ± 1.01	0.46	0.44	0.086
	12 weeks	2.68 ± 0.58	4.79 ± 1.13	2.50 ± 0.95	4.13 ± 1.55	0.28	<b>&lt;0.0001</b>	0.55
Water consumption (ml/24 h)	2 weeks	5.22 ± 2.91	5.70 ± 2.91	4.74 ± 1.24	3.24 ± 1.49	0.12	0.58	0.29
	12 weeks	4.97 ± 8.49	17.70 ± 9.77	2.94 ± 1.80	14.06 ± 10.28	0.35	<b>0.0004</b>	0.79
Urine production (ml/24 h)	2 weeks	0.52 ± 0.34	1.19 ± 0.69	1.34 ± 0.83	0.78 ± 0.91	0.40	0.72	0.081
	12 weeks	1.20 ± 0.76	15.83 ± 8.05	2.03 ± 1.77	12.53 ± 10.84	0.60	<b>&lt;0.0001</b>	0.39
Fasting blood glucose (mmol/L)	12 weeks	9.22 ± 2.72	23.53 ± 3.80	10.10 ± 2.95	19.66 ± 6.94	0.35	<b>&lt;0.0001</b>	0.14
GHb (mmol/mol)	12 weeks	4.22 ± 1.68	7.72 ± 3.79	3.35 ± 0.28	6.86 ± 3.83	0.45	<b>0.0048</b>	0.99

Note: Values are mean ± SD (n = 5–11).

Abbreviations: D, diabetes; G D, interaction; G, genotype; GHb, glycated haemoglobin; STZ, streptozotocin.

Bold values indicate a significant (P < 0.05) effect.

foot processes warranted further investigation of kidney function in *DDOST+/-<sup>Pod-Cre</sup>* mice, to determine whether increasing podocyte expression of OST48 affected glomerular filtration.

### 2.3 | Increases in podocyte OST48 expression decrease GFR, exacerbating DKD

Conscious glomerular filtration rate (GFR), determined as a ratio of subcutaneous excretion of FITC-sinistrin, identified a significant decline in kidney function in *DDOST+/-<sup>Pod-Cre</sup>* mice (Figures 2A–49% decrease, *p* < .0001). Compared to their baseline kidney function, *DDOST+/-<sup>Pod-Cre</sup>* mice lost 59% of GFR over the study period (Figure 2B). Non-diabetic *DDOST+/-<sup>Pod-Cre</sup>* mice also had elevated serum creatinine compared to their wild-type counterparts (Figure 2C—average 88% increase; *p* = .0034), which was further increased by diabetes (Figure 2C—58% increase; *p* = .043 for *DDOST+/-<sup>Pod-Cre</sup>* and 123% increase; *p* = .0047 for wild-type). Diabetes increased serum creatinine in wild-type mice (Figure 2C) and decreased creatinine clearance (Figure 2D), which tended to further decrease in *DDOST+/-<sup>Pod-Cre</sup>* mice, although this did not reach statistical significance (Figure 2D). Compared to wild-type mice, *DDOST+/-<sup>Pod-Cre</sup>* mice averaged a 72% reduction in creatinine clearance following simultaneous blood and 24-hour urine collection (Figure 2E; *p* = .0052) in agreement with FITC-sinistrin based GFR assessment (Figure 2A). Diabetes increased 24-hour urinary albumin excretion rate, but this did not differ between wild-type and *DDOST+/-<sup>Pod-Cre</sup>* mice (Figure 2F and G).

### 2.4 | *DDOST+/-<sup>Pod-Cre</sup>* mice have damaged podocyte architecture and tubulointerstitial damage

Diabetes resulted in glomerulosclerosis in both genotypes (Figure 3A). In the absence of diabetes, *DDOST+/-<sup>Pod-Cre</sup>* mice also had glomerulosclerosis (Figure 3A) and greater glomerular collagen IV accumulation (Figure 3B) than wild-type mice which was not further elevated by diabetes. Glomerular collagen IV accumulation was also present in all diabetic mice (Figure 3B). By electron microscopy, glomerular basement membrane thickening and podocyte foot process effacement were seen in *DDOST+/-<sup>Pod-Cre</sup>*, but not in wild-type mice (Figure 3C). In glomerular fractions from mouse kidney cortices, SWATH-MS proteomics identified significant increases in the abundance of collagen proteins (Figure 3D). Specifically, both diabetes and increased podocyte OST48 expression caused an increased abundance of collagen 1, collagen 6 and other structural collagen proteins (Figure 3D). Given that all *DDOST+/-<sup>Pod-Cre</sup>* mice exhibited a decline in kidney function, we suspected that in addition to damaged glomeruli there would be other structural evidence of progressive kidney damage in the tubules of these mice. As expected, diabetes increased tubulointerstitial fibrosis in WT mice (Figure 4A–C). In addition, there was significant tubulointerstitial fibrosis in all *DDOST+/-<sup>Pod-Cre</sup>* mice compared to wild-type non-diabetic mice, evidenced by an increase in positive connective tissue quantified from Masson's trichrome (Figure 4A), Sirius red (Figure 4B) and collagen IV staining in this compartment (Figure 4C). In tubule-enriched cortical fractions, SWATH-MS proteomics identified modest increases in proteins associated with collagen fibril organization (CO1A1-2)

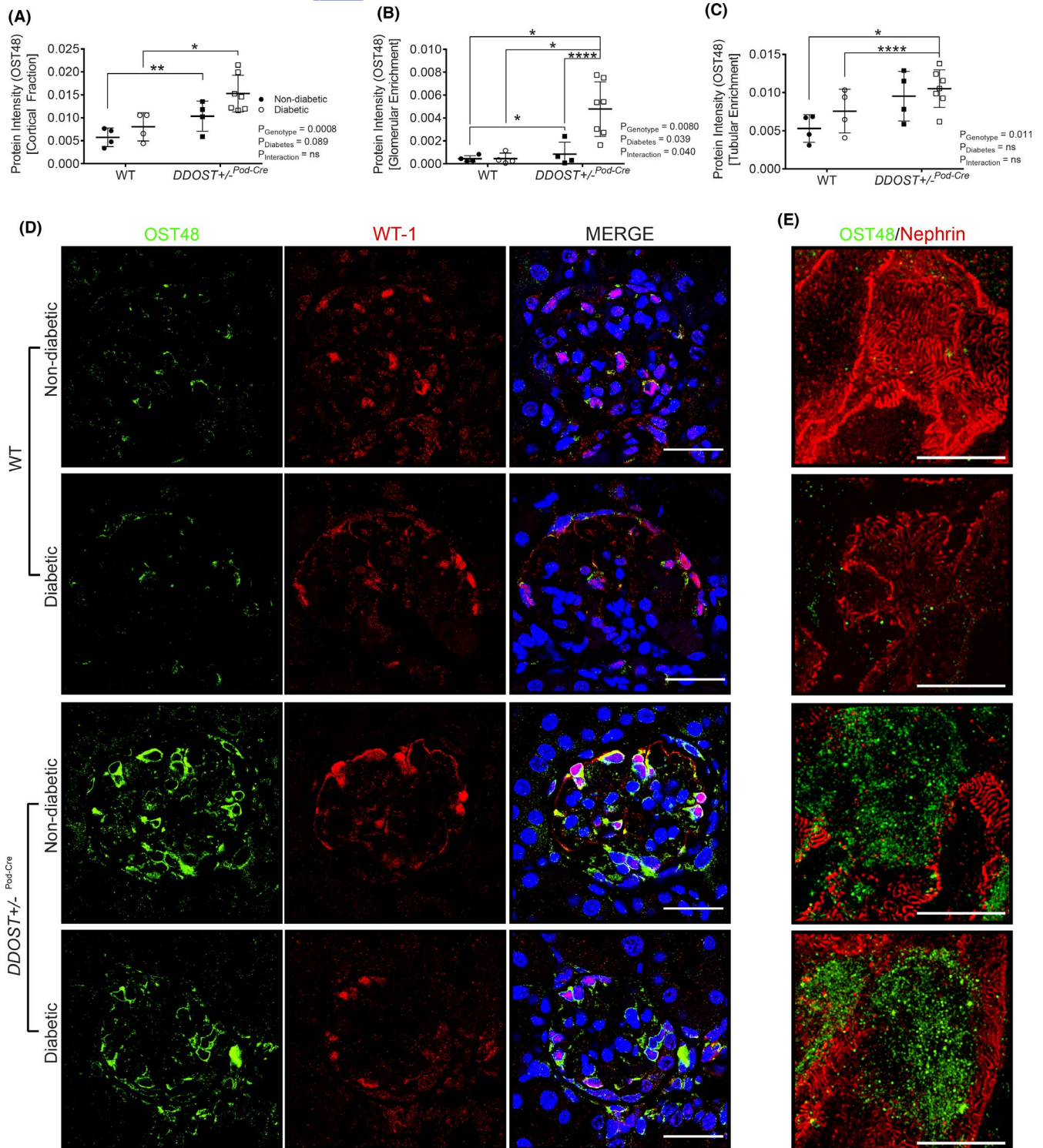


**FIGURE 1** OST48 expression and localization in the kidney at study completion. (A-C) SWATH-MS proteomics quantification of total OST48 in (A) renal cortex and (B-C) enriched for either (B) glomeruli or (C) tubules in both the *DDOST*<sup>+/-</sup>*Pod-Cre* mice and their wild-type littermates. (D) Confocal photomicrographs of OST48 (green) and a podocyte-specific marker WT-1 (red) on kidney sections imaged at the glomerulus. (E) 3DSIM of podocyte foot processes stained with nephrin (red) and OST48 localization (green). Scale bars from representative images for (D) confocal microscopy and (E) 3D-SIM were 30 μm and 5 μm, respectively. Results are expressed as mean ± SD with unpaired t test analysis ( $n = 6-12$ )  $**p < .01$ ,  $***p < .001$  and for proteomics ( $n = 4-6$ ), MSstatsV2.6.4 determined significant changes in the protein intensities  $*p < .05$ ,  $**p < .01$ ,  $****p < .0001$

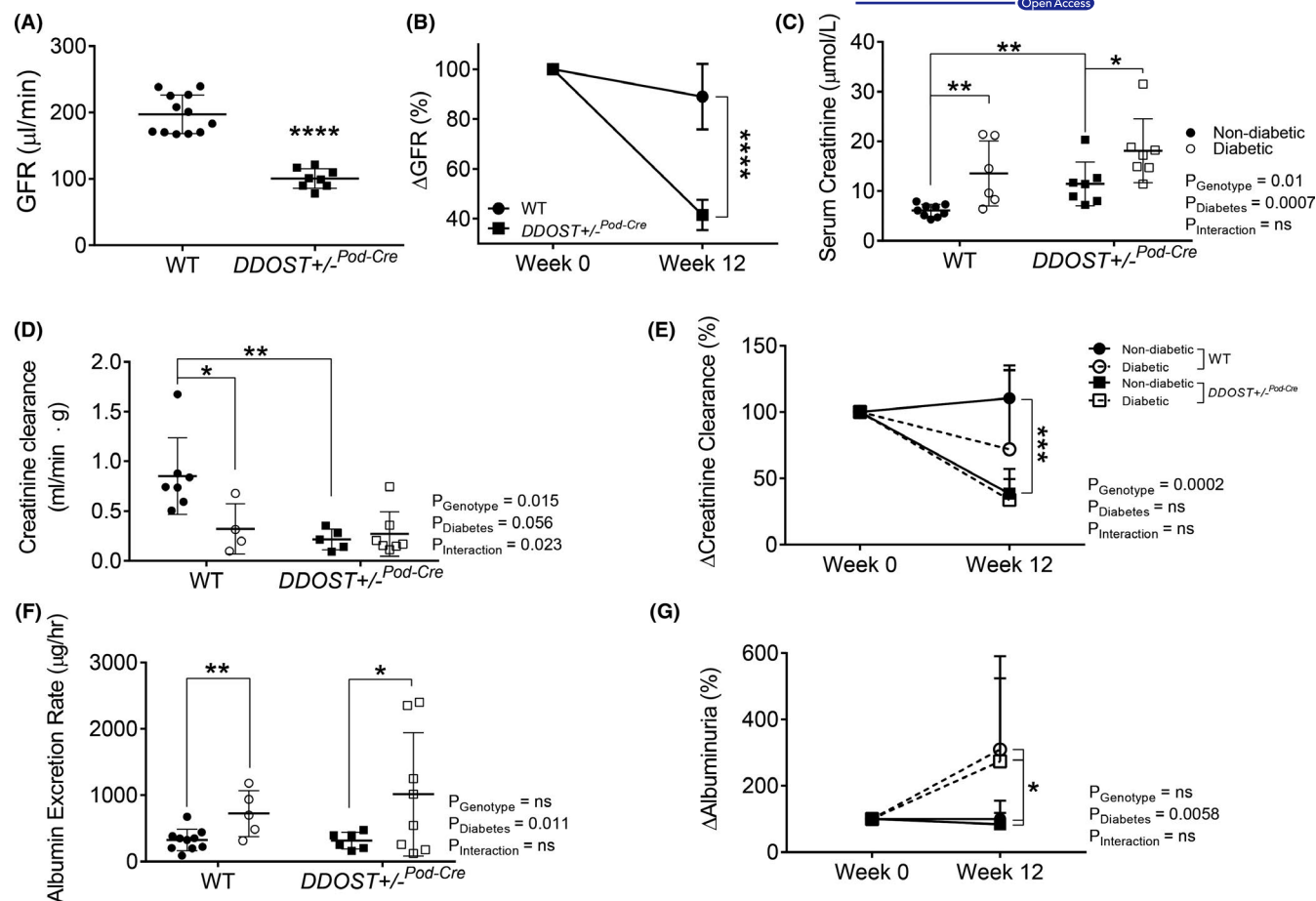


**FIGURE 2** DDOST<sup>+/-</sup>Pod-Cre mice exhibited a rapid and progressive decline in kidney function independent of macroalbuminuria. (A) Calculated GFR using the transcutaneous decay of retro-orbitally injected FITCsinistrin. (B) Change in GFR, which was determined from matched GFR values from week 0 of the study (6–8 weeks of age) to week 12 of the study. Serum and 24-h urine were collected from mice in metabolic cages at week 0 and week 12 of the study. (C–E) Creatinine was measured spectrophotometrically at 550nm in a biochemical analyser. (C) Serum creatinine measured at week 12 of the study. (D) Ratio of creatinine clearance following correction for kidney weight measured at week 12 of the study. (E) Change in creatinine clearance, which was determined from matched creatinine clearance values from week 0 of the study (6–8 weeks of age) to week 12 of the study. (F–G) Albumin was measured spectrophotometrically at 620nm in a biochemical analyser and the albumin excretion rate (AER) was determined based on the 24-hour urine flow rate. (F) AER measured at week 12 of the study. (G) Change in albuminuria over the study, which was determined from matched albuminuria values from week 0 (6–8 weeks of age) of the study to week 12 of the study. Results are expressed as mean ± SD with either two-way ANOVA or paired t-test analysis ( $n = 3–8$ ) \* $p < .05$ , \*\* $p < .01$ , \*\*\* $p < .001$

(Figure 4D) in non-diabetic DDOST<sup>+/-</sup>Pod-Cre mice compared with WT littermates. However, with diabetes, DDOST<sup>+/-</sup>Pod-Cre mice showed a significant accumulation of collagen IV in tubule-enriched fractions not seen in WT diabetic or non-diabetic DDOST<sup>+/-</sup>Pod-Cre mice. There were further modest increases in markers of tubulointerstitial fibrosis in diabetic DDOST<sup>+/-</sup>Pod-Cre but these were not different to WT mice.

## 2.5 | Tissue AGEs were localized to damaged podocytes

Podocyte AGE accumulation and OST48 appeared to be co-localized (Figure 5A) and were prominent in areas where

concomitant deterioration of podocyte foot processes was seen, as defined by loss of both nephrin (Figure 5A) and synaptopodin (Figure S3A). 3D-SIM confirmed the appearance of nodules/vacuoles containing both OST48 and AGEs in DDOST<sup>+/-</sup>Pod-Cre mice in areas of podocyte foot process deterioration (Figure 5B, Figure 5C and Video S2). These changes were not observed in wild-type diabetic mice. Overall, there was a significant reduction in AGE content in kidney cortical extracts taken from DDOST<sup>+/-</sup>Pod-Cre mice (Figure 5D—genotype effect  $p < .05$ ). Diabetes also increased urinary AGE excretion ( $p = .007$ ; ~10-fold increase) when compared to non-diabetic mice (Figure 5E). Although not significant ( $p < .2$ ), there was also a trend towards increased urinary AGE excretion in non-diabetic DDOST<sup>+/-</sup>Pod-Cre mice compared to wild-type non-diabetic mice.

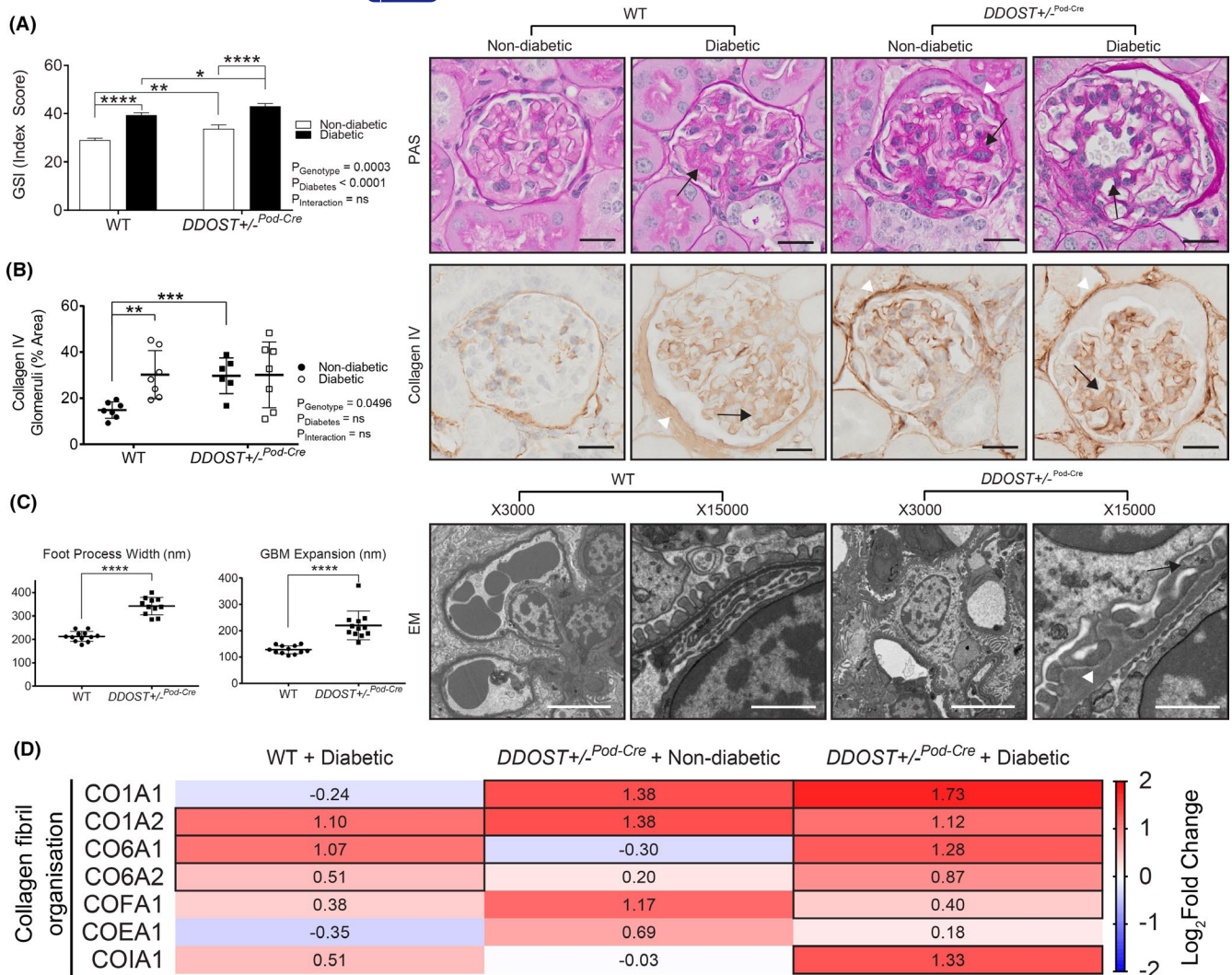


**FIGURE 3** Podocyte OST48 was associated with a deterioration of podocyte architecture. (A–C) Assessment of renal glomerular damage in the kidney with (A) Periodic acid Schiff staining (PAS) and (B) collagen IV, which was then quantified based on a positive threshold protocol. *DDOST*<sup>+/-</sup>*Pod-Cre* mice and mice with a diabetic phenotype show moderate glomerulosclerosis, indicated by an increase in mesangial matrix expansion (black arrow) and accumulation of the extracellular matrix (white arrow head). (C) Electron microscopy determined the degree of hypertrophy in the foot processes (black arrow) and the expansion of the GBM (white arrow head). Scale bars from representative images of (A–B) glomeruli stained with either PAS or collagen IV were 20  $\mu\text{m}$ . (C) Representative images from electron microscopy were imaged at either  $\times 3000$  magnification or  $\times 15000$  magnification were 20  $\mu\text{m}$  and 4  $\mu\text{m}$ , respectively. (D) Heat map representation of SWATH-MS proteomics data for enzymatic pathways involved in collagen fibril organization. Significant proteins are represented as bolded cells, where red indicates an increase and blue indicates a decrease in protein concentrations. Data represented as means  $\pm$  SD ( $n = 4\text{--}7/\text{group}$ ). Results are expressed as mean  $\pm$  SD with either two-way ANOVA or unpaired t-test analysis ( $n = 5\text{--}9$ ) \* $p < .05$ , \*\* $p < .01$ , \*\*\* $p < .001$ , \*\*\*\* $p < .0001$ . For proteomics, MSstatsV2.6.4 determined significant ( $p < .05$ ) log fold changes in the protein intensities between the selected experimental group the wild-type nondiabetic group. Heatmap representation allow for compact visualization of complex data comparisons. Full detail of the quantitative data is available in the supplementary information

## 2.6 | Podocyte OST48-mediated AGE accumulation resulted in ER stress

ER stress at sites of AGE accumulation within damaged podocytes was examined. *DDOST*<sup>+/-</sup>*Pod-Cre* mice exhibited an increase in the ER stress markers GRP-78 and spliced XBP-1 when compared to wild-type mice (Figure 6A). Furthermore, these ER stress markers were further increased by diabetes (Figure 6A). This was confirmed using

SWATH-MS proteomics of glomerular enriched fractions, where diabetic *DDOST*<sup>+/-</sup>*Pod-Cre* mice showed significantly higher abundance of proteins associated with ER stress (GRP75 and GRP78) compared to non-diabetic wild-type mice (Figure 6B). Antioxidant enzymes SOD1/SODC and SOD2/SODM were also increased by diabetes in wild-type mice (Figure 6B). Compared with non-diabetic mice, glomerular fractions from diabetic wild-type and *DDOST*<sup>+/-</sup>*Pod-Cre* mice had significantly higher levels of proteins associated with mitochondrial ATP

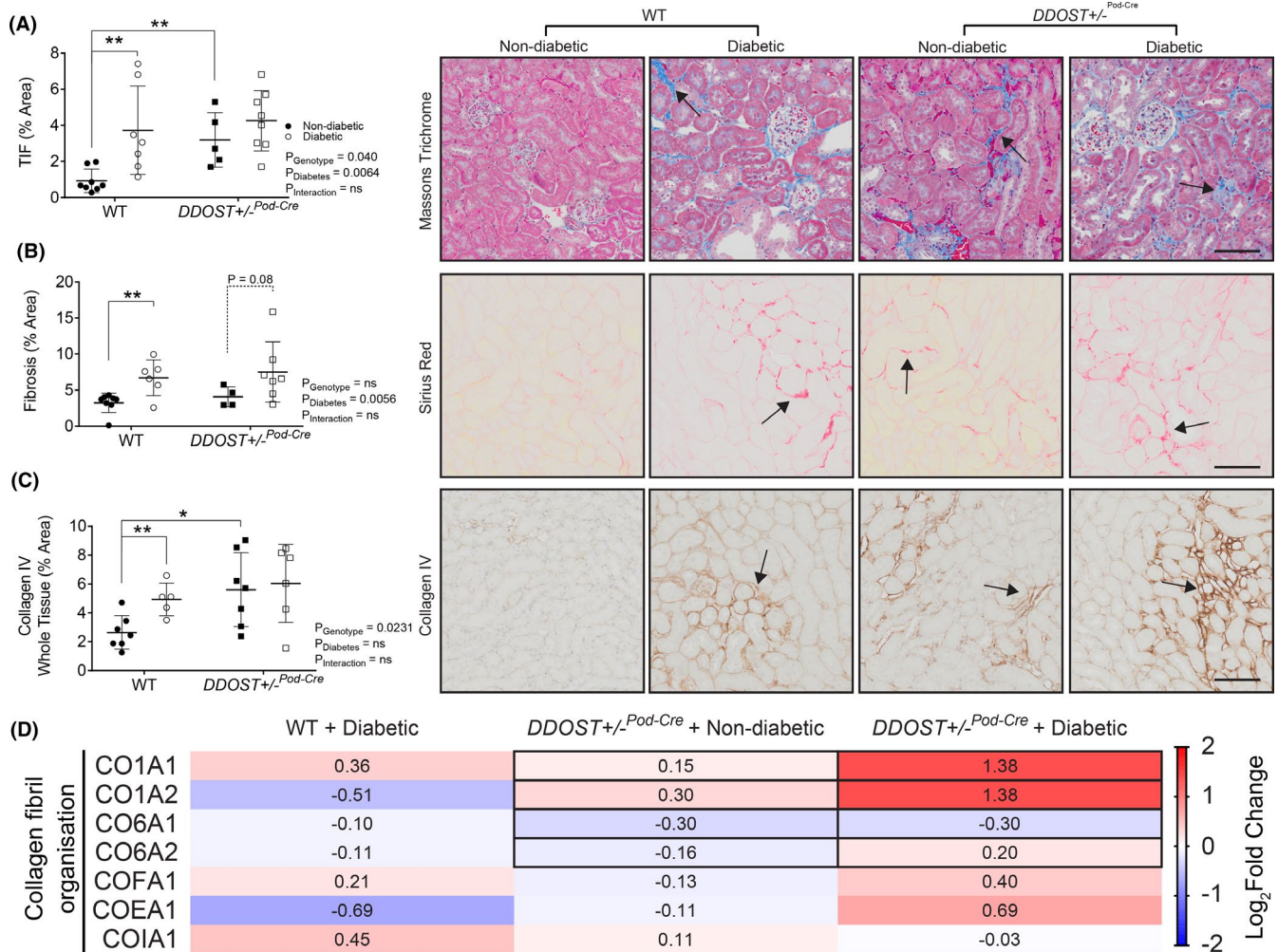


**FIGURE 4** Podocyte OST48 increased tubulointerstitial fibrosis. (A–C) Moreover, the presence of collagen in (A) Masson's trichrome (blue staining), (B) Sirius red (red) and (C) collagen IV (brown) was quantified based on a positive threshold protocol. Fibrosis in the interstitium of the proximal tubules (black arrow) is an indicator of progressive kidney damage. The severity of these changes was more pronounced in the DDOST+/-Pod-Cre mice and the mice with a diabetic phenotype. (D) Heat map representation of SWATH-MS proteomics data for enzymatic pathways involved in collagen fibril organization. Significant proteins are represented as bolded cells, where red indicates an increase and blue indicates a decrease in protein concentrations. Data represented as means  $\pm$  SD ( $n = 4\text{--}7/\text{group}$ ). Scale bars from representative images of (A–C) proximal tubule sections stained with either Masson's trichrome, Sirius red or collagen IV were 100  $\mu\text{m}$ . Results are expressed as mean  $\pm$  SD with either two-way ANOVA or unpaired t test analysis ( $n = 5\text{--}9$ ) \* $p < .05$ , \*\* $p < .01$ . For proteomics, MSstatsV2.6.4 determined significant ( $p < .05$ ) log fold changes in the protein intensities between the selected experimental group the wild-type non-diabetic group. Heatmap representation allow for compact visualization of complex data comparisons. Full detail of the quantitative data is available in the supplementary information

synthesis, particularly biosynthesis of complex I components (NADH dehydrogenase:ubiquinone) (Figure 6C).

### 3 | DISCUSSION

Lowering AGE burden, including by facilitating renal AGE clearance, has been suggested as a possible treatment for DKD. However, the assertion that increasing renal AGE clearance receptors such as OST48 may protect against DKD has not been previously investigated. Here, we have shown for the first time that increasing OST48 in a podocyte-specific manner decreased glomerular filtration and

caused podocyte structural damage including foot process effacement, leading to glomerulosclerosis and tubulointerstitial fibrosis, and some parameters were further exacerbated by diabetes. Surprisingly, in non-diabetic mice the decline in GFR and increased podocyte and glomerular damage were seen in the absence of elevations in albuminuria. Mechanistically, increases in OST48 in podocytes were marked by increased podocyte-specific AGE uptake resulting in oxidative and endoplasmic reticulum stress, which is independent of changes to the N-glycosylation machinery and subsequent kidney functional and structural decline (Figure 7), where previously it has been shown that AGE uptake into cultured podocytes induces hypertrophy<sup>41</sup> and apoptosis.<sup>42</sup>

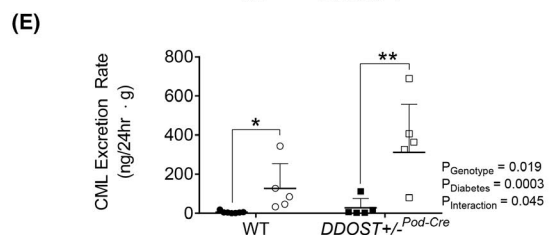
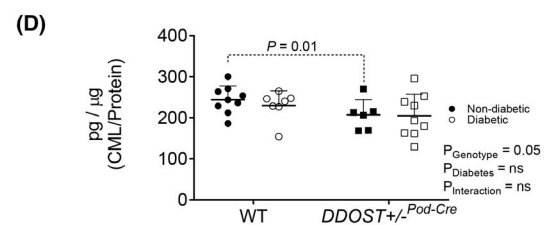
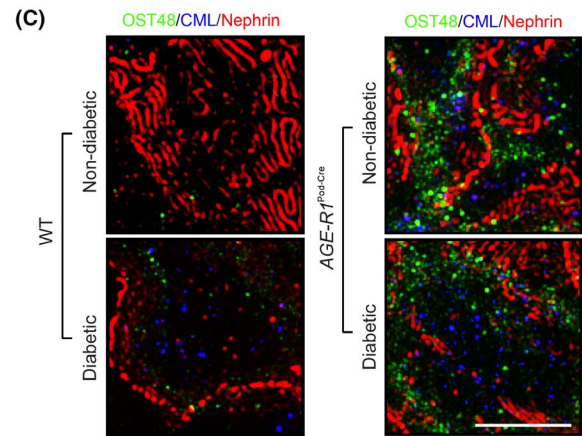
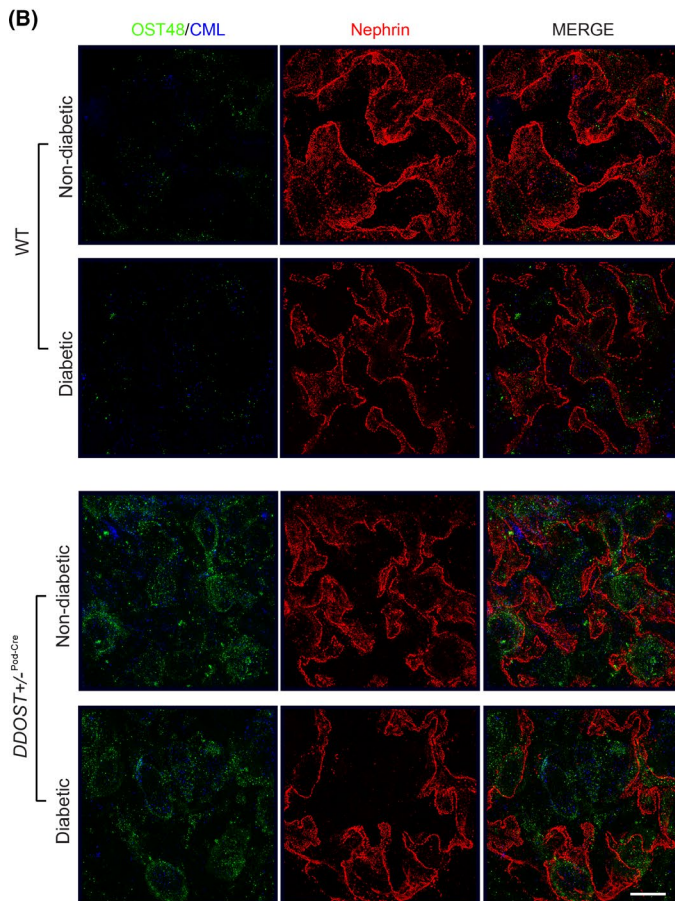
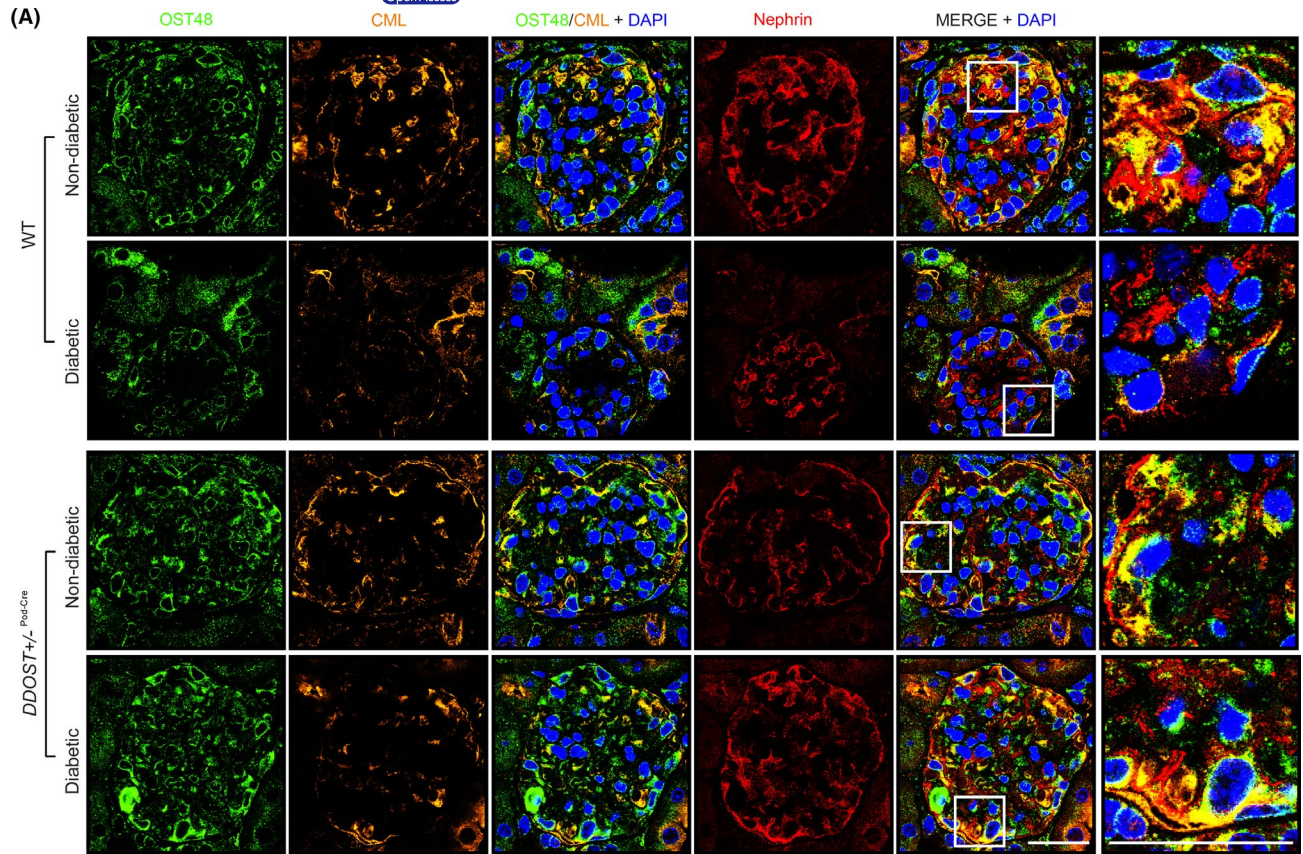




**FIGURE 5** Podocyte OST48 increased AGE accumulation in podocytes. (A) Confocal photomicrographs of OST48 (green), CML (orange) and a podocyte foot process marker, nephrin (red) on kidney sections imaged at a glomerulus. (B) 3D-SIM of podocyte foot processes staining for nephrin (red), OST48 (green) and CML (blue) localization. (C) 3D-SIM reconstruction of podocyte foot processes staining for nephrin (red), OST48 (green) and CML (blue) localization. (D-E) CML ELISA measuring the total content of CML detected in (D) whole kidney cortex homogenates and in (E) 24-hour urine collections. Scale bars from representative images for (A) confocal microscopy and (B-C) 3D-SIM were 30  $\mu\text{m}$  and 5  $\mu\text{m}$ , respectively. Results are expressed as mean  $\pm$  SD with either two-way ANOVA or unpaired *t* test analysis ( $n = 5-9$ ) \* $p < .05$

It was particularly interesting that albuminuria was not seen concomitantly with the loss of GFR in non-diabetic  $DDOST^{+/-Pod-Cre}$  mice despite podocyte foot effacement, thickening of the glomerular basement membrane and glomerulosclerosis. Although surprising, this is consistent with clinical observations. For example, the prospective longitudinal Joslin Proteinuria Cohort studies<sup>46,47</sup> identified that the overall prevalence of normo-albuminuria in patients with progressive kidney disease was around 10% and that regression from micro- and macro-albuminuria to normo-albuminuria was repeatedly observed. We observed podocyte foot effacement and glomerular basement membrane thickening, which are commonly attributed as causes of micro- and macro-albuminuria. This finding is consistent with other postulated models of the origins of albuminuria, such as the high glomerular sieving coefficient (GSC) hypothesis.<sup>48,49</sup> This hypothesis suggests that albuminuria is driven by proximal tubule damage which prevents the reabsorption/processing of albumin by these cells. In support of this model, tubulointerstitial fibrosis was more pronounced in diabetic mice regardless of their genotype, and they also had concomitant increases in urinary albumin excretion which not seen in non-diabetic mice. Alternatively, the absence of macro-albuminuria seen in mice with increased podocyte expression of OST48 could be attributed to the significant decline in GFR, as this would limit the flux of albumin into the urine.

Although we showed that increases in podocyte OST48 expression decreased renal AGE accumulation and increased urinary AGE excretion, this was not associated with reno-protection. In fact, this resulted in significant renal disease. We have shown for the first time that OST48 and AGEs colocalize within podocytes, in areas of foot process denudation and damage. We observed that OST48 facilitation of podocyte AGE accumulation resulted in a cascade of ER stress and mitochondrial abnormalities, culminating in podocyte foot process effacement, GBM expansion and renal functional decline. Increasing the urinary flux of AGEs has indeed been previously shown to impair renal function in both healthy humans<sup>43,50</sup> and early in the development of diabetic kidney disease in rodent models.<sup>37,51</sup> This is interesting given that although AGE accumulation is facilitated and accelerated by the hyperglycaemia of diabetes, there is substantial evidence that AGE accumulation is a pathological mediator of many chronic kidney diseases, where AGE formation is driven by oxidative stress, dyslipidaemia, uraemia and insulin resistance independent to diabetes.<sup>43,52</sup> In those instances, AGEs have a major contribution to pathology including podocyte loss, where that chronic AGE administration can mimic chronic kidney disease in the absence of diabetes. Therefore, we believe that AGE accumulation in the podocytes is sufficient to drive kidney disease in the absence

of diabetes, while strategies to decrease AGEs in chronic kidney disease can improve kidney function.

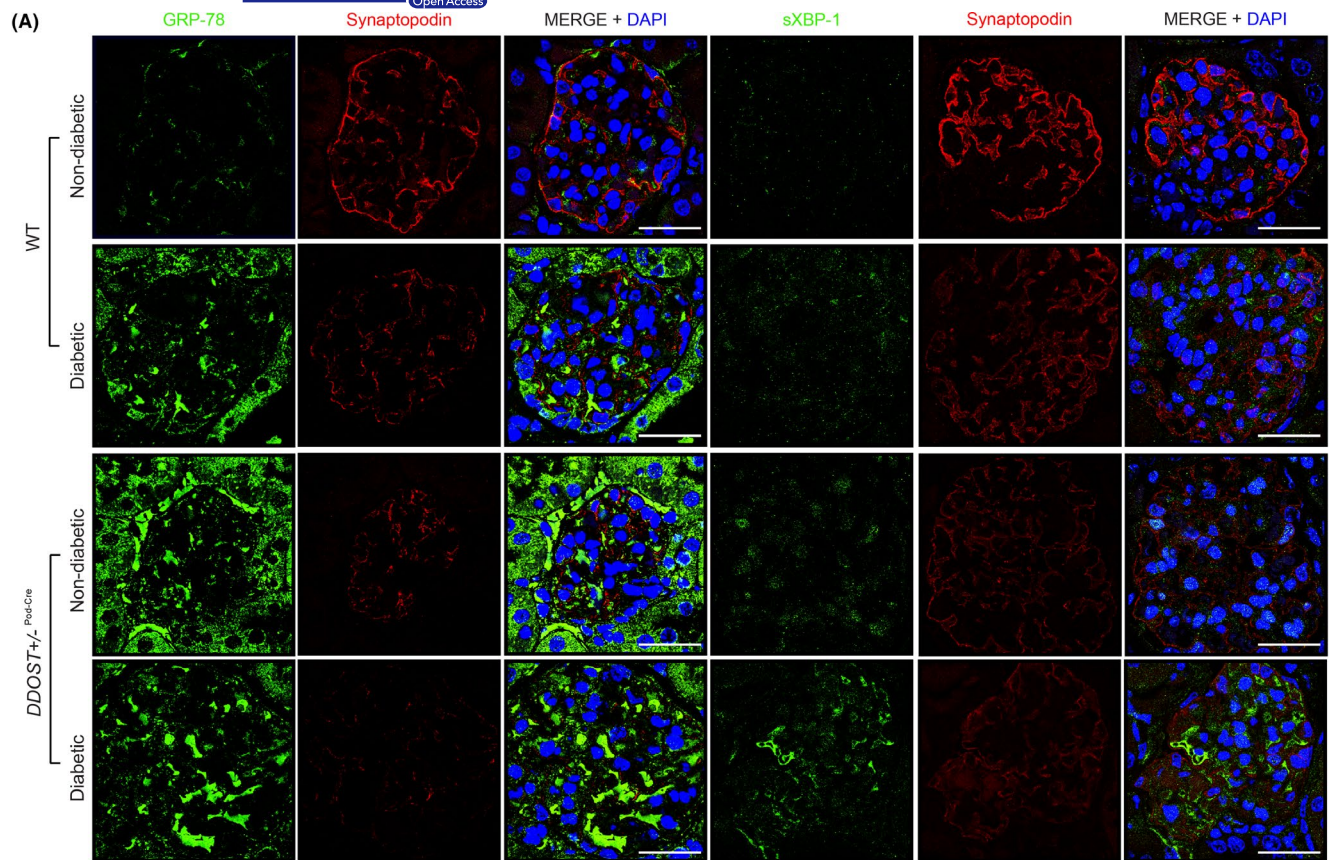
Interestingly, OST48 over-expression contributed most to the physiological decline in kidney function measured as GFR, with modest additive effects seen with diabetes induction. A limitation of our podocyte-specific over-expression model is that it is present during *in utero* development which may explain the predominant physiological impact of OST48 in the absence of diabetes. In the future, an inducible model where OST-48 can be over-expressed once diabetes is established, may better delineate any combined effects of OST48 and diabetes-induced hyperglycaemia on kidney function. 1.7-fold in the tubular compartment. Another limitation is that control mice with diabetes exhibited kidney damage indicative of moderate diabetic kidney disease, which was more pronounced than the early-stage kidney disease usually seen following diabetes induction with STZ in C57BL/6J mice. It is important to note that control mice in the present study were the WT/WT littermates of  $DDOST^{+/-Pod-Cre}$  (WT/het) mice and therefore *in utero*, control WT/WT fetuses were gestated with  $DDOST^{+/-Pod-Cre}$  (WT/het) fetuses. Hence, we postulate that the altered susceptibility to diabetic kidney disease seen in the control WT/WT mice given STZ in this study was due to their *in utero* environment, since we controlled for any non-specific disruption by our genetic modifications by removing the neo delivery cassette for the transgene and targeting insertion of the DNA into the ROSA 26 locus, underwent extensive backcrossing to the C57BL/6J background and ensured mice from the same litters were randomized mice to different groups.

Taken together, these results suggest that specifically increasing podocyte exposure and uptake of AGEs thereby facilitating their flux into the urine is sufficient to induce significant kidney damage. Moreover, it should be noted that modulation of surface AGE receptors on podocytes to facilitate excretion may not be an optimal target to improve DKD due to the consequential effects of podocyte effacement.

## 4 | METHODS

### 4.1 | Animals

All animal studies were performed in accordance with guidelines provided by the AMREP (Alfred Medical Research and Education Precinct) Animal Ethics Committee, University of Queensland and the National Health and Medical Research Council of Australia (E/1184/2012/B and MRI-UQ/TRI/256/15/KHA). Male C57BL/6J wild-type mice with a genetic insertion of the human



(B)

	WT + Diabetic	<i>DDOST</i> <sup>+/-Pod-Cre</sup> + Non-diabetic	<i>DDOST</i> <sup>+/-Pod-Cre</sup> + Diabetic		
BIP proteins	GRP78	0.22	0.01	0.49	Log <sub>2</sub> Fold Change
	GRP75	0.15	0.55	0.09	
OS proteins	TERRA	-0.07	0.05	0.57	
	SODC	0.76	0.48	-0.11	
	SODM	0.72	0.11	0.27	

(C)

	WT + Diabetic	<i>DDOST</i> <sup>+/-Pod-Cre</sup> + Non-diabetic	<i>DDOST</i> <sup>+/-Pod-Cre</sup> + Diabetic	
Ubiquinone biosynthesis proteins	NDUA7	1.53	0.02	0.33
	NDUA8	1.03	2.99e-004	0.32
	NDUA9	0.67	0.44	1.46
	NDUAA	0.08	-3.01e-003	0.42
	NDUAD	0.83	0.07	0.53
	NDUB3	0.98	0.41	1.03
	NDUB5	0.10	0.13	1.62
	NDUC2	0.58	-0.55	0.68
	NDUS1	0.13	-0.28	0.87
	NDUS2	0.58	0.91	1.43
	NDUS3	0.42	0.35	1.13
	NDUS7	0.02	0.13	0.49
	NDUS8	0.26	0.10	0.53
	NDUV1	-0.01	0.22	0.47
	NDUV2	0.26	-0.86	0.97
	COQ9	-0.36	0.01	-0.80

**FIGURE 6** Podocyte OST48 increased ER stress markers. (A) Confocal photomicrographs of either ER stress marker GRP-78 (green), or XBP-1 (green) and podocyte foot process marker, synaptopodin (red). (B-C) Heat map representation of SWATH-MS proteomics data for enzymatic pathways involved in (B) endoplasmic reticulum (ER) stress and oxidative stress (OS) enzymatic pathways, and (C) ubiquinone biosynthesis pathways. Significant proteins are represented as bolded cells, where red indicates an increase and blue indicates a decrease in protein concentrations. Data represented as means  $\pm$ SD ( $n = 4$ -7/group). Scale bars from representative images of confocal microscopy were 30  $\mu$ m. Data represented as means  $\pm$ SD ( $n = 5$ /group). For proteomics, MSstatsV2.6.4 determined significant ( $p < .05$ ) log fold changes in the protein intensities between the selected experimental group the wild-type non-diabetic group. Heatmap representation allow for compact visualization of complex data comparisons. Full detail of the quantitative data is available in the supplementary information

gene encoding AGE-R1/OST-48 (*DDOST*) in the *ROSA26* locus (*ROSA26<sup>tm1(DDOST)Jfo</sup>*) crossed with mice only expressing *Cre* under the control of the *Podocin* promoter (termed *DDOST<sup>+/-Pod-Cre</sup>*) were generated (Figure S1A) by Ozgene Australia (Ozgene). Between 6 and 8 weeks of age (Week 0), experimental diabetes (DIAB) was induced in male *DDOST<sup>+/-Pod-Cre</sup>* ( $n = 10$ ) and wild-type ( $n = 9$ ) littermate mice by low dose intraperitoneal injection of streptozotocin.<sup>53</sup> Non-diabetic male *DDOST<sup>+/-Pod-Cre</sup>* ( $n = 7$ ) and wild-type ( $n = 11$ ) mice received equivalent injections of sodium citrate buffer alone. After 10 days of recovery, blood glucose concentrations were determined and then repeated weekly to ensure mice had diabetes ([blood glucose] $>15$ mmol/L). Mice were allowed access to food and water *ad libitum* and were maintained on a 12-hour light:dark cycle at 22°C. All mice received a diet of standard mouse chow (AIN-93G) (Specialty Feeds, Glen Forrest). At 0 and 12 weeks of the study, mice were housed in metabolic cages (Iffa Credo) for 24 h to determine food and water consumption and collect urine. Urine output was also measured during caging and urinary glucose determined by a glucometer (SensoCard Plus, POCD).

## 4.2 | Glomerular and tubule enrichment

Kidneys were decapsulated and the medulla discarded. Cortex was kept cold, minced and passed gently through first a 250  $\mu$ m sieve and then a 75  $\mu$ m sieve. Tubular-enriched proteins were contained in the elute while the glomerular-enriched proteins were located on the top of the 75  $\mu$ m sieve. Enriched proteins were collected and processed for mass spectrometry analysis. Glomerular- (SYNPO, ACTN4) and tubular-specific (AQP1, DIC, S22A6) proteins were significantly enriched in respective fractions (Figure S1C).

## 4.3 | Biochemical analyses

$N_{\epsilon}$ -(Carboxymethyl)lysine (CML) concentrations in plasma and urine were measured by an in-house indirect ELISA as previously described.<sup>30</sup> Urinary albumin (Bethyl Laboratories, United States) was normalized to the 24-h flow rate of urine. Serum and urinary creatinine were measured spectrophotometrically at 505 nm (Roche/Hitachi 902 Analyzer, Roche Diagnostics GmbH) using the Jaffe method.

## 4.4 | Glomerular filtration rate

At 0 and 12 weeks of the study, GFR was estimated in conscious mice using the transcutaneous decay of retro-orbitally injected FITC-sinistrin (10 mg/100 g body weight dissolved in 0.9% NaCl), as previously described.<sup>54</sup> GFR was calculated from the rate constant ( $\alpha_2$ ) of the single exponential excretion phase of the curve and a semi-empirical factor.

## 4.5 | Liquid chromatography-tandem mass spectrometry proteomics

Fractions enriched for either glomeruli or tubules were processed as previously described.<sup>55</sup> Peptides were desalted and analysed by Information Dependent Acquisition Liquid chromatography-tandem mass spectrometry (LC-MS/MS) as described<sup>56</sup> using a Prominence nanoLC system (Shimadzu,) and Triple TOF 5600 mass spectrometer with a Nanospray III interface (AB SCIEX). SWATH-MS analysis was performed<sup>57</sup> and differentially abundant proteins were analysed using DAVID.<sup>58</sup> Processed proteomic data sets are available in the Supplementary Information.

## 4.6 | Histology and imaging

Paraffin-embedded sections were stained with either a Periodic acid Schiff (PAS) staining kit (Sigma-Aldrich), a Trichrome (Masson) staining kit (Sigma-Aldrich) or Sirius Red (Sigma-Aldrich). Collagen IV was determined by immunohistochemistry using an anti-collagen IV antibody (1:100 dilution; ab6586; Abcam). All sections were visualized on an Olympus Slide scanner VS120 (Olympus) and viewed in the supplied program (OlyVIA Build 10555, Olympus). Slides were quantified based on threshold analysis in Fiji.<sup>59</sup> Briefly, for immunofluorescence staining, frozen kidney sections were stained with a combination of either anti-CML (1:200 dilution; ab27684; Abcam), OST48 (H-1; 1:100 dilution; SC-74408; Santa Cruz biotechnologies), GRP78 (A-10; 1:50 dilution; SC-376768; Santa Cruz biotechnologies), WT-1 (c-terminus; 1:100 dilution; PA5-16879; Thermo Fisher Scientific), synaptopodin (P-19; 1:100 dilution; SC-21537; Santa Cruz biotechnologies), nephrin (1:100 dilution; ab27684; Abcam). Confocal images were visualized on an Olympus FV1200 confocal microscope (Olympus) and viewed in the supplied program (FV10,

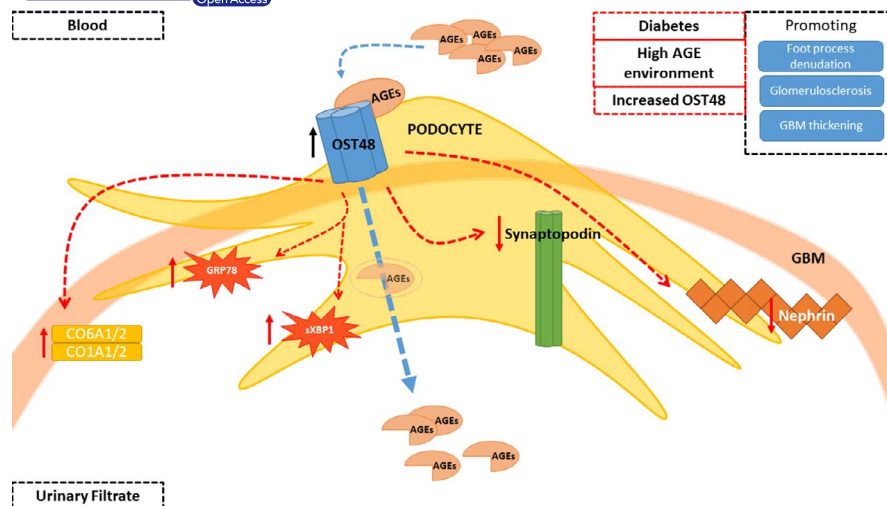


**FIGURE 7** Podocyte OST48 drives podocyte foot process effacement. (A) Working diagram depicting the model whereby OST48 drives podocyte foot process effacement in a streptozotocin-induced model of DKD. AGEs; advanced glycation end products, GBM; glomerular basement membrane, OST48; advanced glycation end-product receptor 1/oligosaccharyltransferase-48 kDa subunit, GRP78; 78 kDa glucose-regulated protein/binding immunoglobulin protein, sXBP1; spliced X-box binding protein 1; CO6A1/2; collagen alpha-1/2 (VI) chain; CO1A1/2; collagen alpha-1/2 (I) chain

Olympus). For ultra-resolution 3D microscopy, slides were visualized on an OMX Blaze deconvolution structured illumination (SIM) super-resolution microscope (GE Healthcare Life Science).

#### 4.7 | Glomerulosclerotic index

Glomerulosclerotic index (GSI) as a measure of glomerular fibrosis was evaluated in a blinded manner by a semi-quantitative method.<sup>60</sup> Severity of glomerular damage was assessed on the following parameters; mesangial matrix expansion and/or hyalinosis of focal adhesions, true glomerular tuft occlusion, sclerosis and capillary dilation.

#### 4.8 | Fixation, tissue processing and acquisition of data from electron microscopy

Renal cortex was processed as previously described.<sup>61</sup> Sections were cut at 60nm on a Leica UC6 ultramicrotome (Leica) and were imaged at 80 kV on a Jeol JSM 1011 transmission electron microscope (Jeol) equipped with an Olympus Morada (Olympus, Japan) digital camera. Quantification of foot process width and GBM expansion was assessed as previously described.<sup>62</sup>

#### 4.9 | Statistics

Results are expressed as mean  $\pm$  SD (standard deviation) and assessed in GraphPad Prism V7.01 for Windows (GraphPad Software). Normally distributed parameters (tested with D'Agostino & Pearson

omnibus normality test) were tested for statistical significance by 2-way ANOVA followed by post hoc testing for multiple comparisons using the Bonferroni method unless otherwise specified. For comparison between groups as required, a two-tailed unpaired Student's *t* test was used where specified. For SWATH-MS, MSstatsV2.6.4<sup>63</sup> was used to detect differentially abundant proteins estimating the log-fold changes between compared conditions of the chosen experimental group and with the wild-type non-diabetic mice. For all calculations, a  $p < 0.05$  was considered as statistically significant. The primary endpoint kidney function. Six mice/group will be required to observe a 10% change in eGFR ( $\alpha = .05$ , power = 0.9 and SD = 0.1). Animal studies and statistical analysis were blinded under the ARRIVE guidelines.

#### ACKNOWLEDGEMENTS

The authors acknowledge the Translational Research Institute (TRI) for providing the excellent research environment and core facilities that enabled this research. We particularly thank Sandrine Roy and Ali Ju from the TRI Microscopy Core Facility. Furthermore, the authors acknowledge the assistance in electron microscopy provided by Jennifer Brown from the Centre for Microscopy and Microanalysis at the University of Queensland.

#### DISCLOSURE

J.M.F. is supported by a Senior Research Fellowship (APP1004503;1102935) from the National Health and Medical Research Council of Australia (NHMRC). B.L.S. is supported by a Career Development Fellowship (APP1087975) from the NHMRC. A.Z. received a scholarship from Kidney Health Australia (SCH17; 141516) and the Mater Research Foundation. M.T.C. is supported by a Career Development Fellowship from the Australian Type

1 Diabetes Clinical Research Network, a special initiative of the Australian Research Council. This research was supported by the NHMRC, Kidney Health Australia and the Mater Foundation, which had no role in the study design, data collection and analysis, decision to publish, or preparation or the manuscript.

#### AUTHOR CONTRIBUTIONS

A.Z., B.L.S. and J.M.F. designed the study. A.Z., F.Y.T, D.J.B, S.L., M.T.C., K.C., D.M. and S.A.P. carried out the experiments. A.Z., B.L.S. and J.M.F. analysed the data. A.Z., B.L.S. and J.M.F. made the figures. A.Z., B.L.S. and J.M.F. drafted and revised the paper. D.M., K.C.S. and M.T.C. assisted with revision of the paper. All authors approved the final version of the manuscript.

#### DATA AVAILABILITY STATEMENT

The data sets generated and analysed during the current study are available from the corresponding author upon reasonable request. The mass spectrometry proteomics data have been deposited to the ProteomeXchange Consortium via the PRIDE<sup>64</sup> partner repository with the data set identifier PXD011434.

#### ORCID

Aowen Zhuang  <https://orcid.org/0000-0002-7409-6629>

Danielle J. Borg  <https://orcid.org/0000-0001-6126-7583>

Josephine M. Forbes  <https://orcid.org/0000-0002-5595-8174>

#### REFERENCES

- Shaw JE, Sicree RA, Zimmet PZ. Global estimates of the prevalence of diabetes for 2010 and 2030. *Diabetes Res Clin Pract.* 2010;87(1):4-14.
- Danaei G, Finucane MM, Lu Y, et al. National, regional, and global trends in fasting plasma glucose and diabetes prevalence since 1980: systematic analysis of health examination surveys and epidemiological studies with 370 country-years and 2.7 million participants. *Lancet.* 2011;378(9785):31-40.
- Gerstein HC, Pogue J, Mann JF, et al. The relationship between dysglycaemia and cardiovascular and renal risk in diabetic and non-diabetic participants in the HOPE study: a prospective epidemiological analysis. *Diabetologia.* 2005;48(9):1749-1755.
- Fox CS, Coady S, Sorlie PD, et al. Increasing cardiovascular disease burden due to diabetes mellitus: the Framingham Heart Study. *Circulation.* 2007;115(12):1544-1550.
- Matsushita K, van der Velde M, Astor BC, et al. Association of estimated glomerular filtration rate and albuminuria with all-cause and cardiovascular mortality in general population cohorts: a collaborative meta-analysis. *Lancet (London, England).* 2010;375(9731):2073-2081.
- Kshirsagar AV, Joy MS, Hogan SL, Falk RJ, Colindres RE. Effect of ACE inhibitors in diabetic and nondiabetic chronic renal disease: a systematic overview of randomized placebo-controlled trials. *Am J Kidney Dis.* 2000;35(4):695-707.
- Fu MX, Wells-Knecht KJ, Blackledge JA, et al. and cross-linking of collagen by glucose. Kinetics, mechanisms, and inhibition of late stages of the Maillard reaction. *Diabetes.* 1994;43(5):676-683.
- Horie K, Miyata T, Maeda K, et al. Immunohistochemical colocalization of glycoxidation products and lipid peroxidation products in diabetic renal glomerular lesions. Implication for glycoxidative stress in the pathogenesis of diabetic nephropathy. *J Clin Investig.* 1997;100(12):2995-3004.
- Monnier VM, Bautista O, Kenny D, et al. Skin collagen glycation, glycoxidation, and crosslinking are lower in subjects with long-term intensive versus conventional therapy of type 1 diabetes: relevance of glycated collagen products versus HbA1c as markers of diabetic complications. DCCT Skin Collagen Ancillary Study Group. *Diabetes Control and Complications Trial. Diabetes.* 1999;48(4):870-880.
- Genuth S, Sun W, Cleary P, et al. Skin advanced glycation end products glucosepane and methylglyoxal hydroimidazolone are independently associated with long-term microvascular complication progression of type 1 diabetes. *Diabetes.* 2015;64(1):266-278.
- Genuth S, Sun W, Cleary P, et al. Glycation and carboxymethyllysine levels in skin collagen predict the risk of future 10-year progression of diabetic retinopathy and nephropathy in the diabetes control and complications trial and epidemiology of diabetes interventions and complications participants with type 1 diabetes. *Diabetes.* 2005;54(11):3103-3111.
- Monnier VM, Sun W, Gao X, et al. Skin collagen advanced glycation endproducts (AGEs) and the long-term progression of sub-clinical cardiovascular disease in type 1 diabetes. *Cardiovasc Diabetol.* 2015;14:118.
- Nin JW, Jorsal A, Ferreira I, et al. Higher plasma levels of advanced glycation end products are associated with incident cardiovascular disease and all-cause mortality in type 1 diabetes: a 12-year follow-up study. *Diabetes Care.* 2011;34(2):442-447.
- Hanssen NM, Beulens JW, van Dieren S, et al. Plasma advanced glycation end products are associated with incident cardiovascular events in individuals with type 2 diabetes: a case-cohort study with a median follow-up of 10 years (EPIC-NL). *Diabetes.* 2015;64(1):257-265.
- Koschinsky T, He CJ, Mitsuhashi T, et al. Orally absorbed reactive glycation products (glycotoxins): an environmental risk factor in diabetic nephropathy. *Proc Natl Acad Sci USA.* 1997;94(12):6474-6479.
- He C, Sabol J, Mitsuhashi T, Vlassara H. Dietary glycotoxins: inhibition of reactive products by aminoguanidine facilitates renal clearance and reduces tissue sequestration. *Diabetes.* 1999;48(6):1308-1315.
- Rigalleau V, Cournard-Gregoire A, Nov S, et al. Association of advanced glycation end products and chronic kidney disease with macroangiopathy in type 2 diabetes. *J Diabetes Complications.* 2015;29(2):270-274.
- Meerwaldt R, Zeebregts CJ, Navis G, Hillebrands JL, Lefrandt JD, Smit AJ. Accumulation of advanced glycation end products and chronic complications in ESRD treated by dialysis. *Am J Kidney Dis.* 2009;53(1):138-150.
- Williams ME, Bolton WK, Khalifah RG, Degenhardt TP, Schotzinger RJ, McGill JB. Effects of pyridoxamine in combined phase 2 studies of patients with type 1 and type 2 diabetes and overt nephropathy. *Am J Nephrol.* 2007;27(6):605-614.
- Freedman BI, Wuerth JP, Cartwright K, et al. Design and baseline characteristics for the aminoguanidine Clinical Trial in Overt Type 2 Diabetic Nephropathy (ACTION II). *Control Clin Trials.* 1999;20(5):493-510.
- Nenna A, Nappi F, Avtaar Singh SS, et al. Pharmacologic approaches against advanced glycation end products (AGEs) in diabetic cardiovascular disease. *Res Cardiovasc Med.* 2015;4(2):e26949.
- Silberstein S, Kelleher DJ, Gilmore R. The 48-kDa subunit of the mammalian oligosaccharyltransferase complex is homologous to the essential yeast protein WBP1. *J Biol Chem.* 1992;267(33):23658-23663.
- Li YM, Mitsuhashi T, Wojciechowicz D, et al. Molecular identity and cellular distribution of advanced glycation endproduct receptors: relationship of p60 to OST-48 and p90 to 80K-H membrane proteins. *Proc Natl Acad Sci USA.* 1996;93(20):11047-11052.

24. Stitt AW, Li YM, Gardiner TA, Bucala R, Archer DB, Vlassara H. Advanced glycation end products (AGEs) co-localize with AGE receptors in the retinal vasculature of diabetic and of AGE-infused rats. *Am J Pathol.* 1997;150(2):523-531.
25. Uhlen M, Fagerberg L, Hallstrom BM, et al. Proteomics. Tissue-based map of the human proteome. *Science (New York, NY).* 2015;347(6220):1260419.
26. Vlassara H, Brownlee M, Cerami A. Novel macrophage receptor for glucose-modified proteins is distinct from previously described scavenger receptors. *J Exp Med.* 1986;164(4):1301-1309.
27. He CJ, Koschinsky T, Buenting C, Vlassara H. Presence of diabetic complications in type 1 diabetic patients correlates with low expression of mononuclear cell AGE-receptor-1 and elevated serum AGE. *Mol Med (Cambridge, Mass).* 2001;7(3):159-168.
28. Ponten F, Gry M, Fagerberg L, et al. A global view of protein expression in human cells, tissues, and organs. *Mol Syst Biol.* 2009;5:337.
29. Cai W, He JC, Zhu L, Lu C, Vlassara H. Advanced glycation end product (AGE) receptor 1 suppresses cell oxidant stress and activation signaling via EGF receptor. *Proc Natl Acad Sci USA.* 2006;103(37):13801-13806.
30. Coughlan MT, Thallas-Bonke V, Pete J, et al. Combination therapy with the advanced glycation end product cross-link breaker, alagebrium, and angiotensin converting enzyme inhibitors in diabetes: synergy or redundancy? *Endocrinology.* 2007;148(2):886-895.
31. Stitt AW, Burke GA, Chen F, McMullen CB, Vlassara H. Advanced glycation end-product receptor interactions on microvascular cells occur within caveolin-rich membrane domains. *FASEB J.* 2000;14(15):2390-2392.
32. Sever S, Altintas MM, Nankoe SR, et al. Proteolytic processing of dynamin by cytoplasmic cathepsin L is a mechanism for proteinuric kidney disease. *J Clin Investig.* 2007;117(8):2095-2104.
33. Yanagida-Asanuma E, Asanuma K, Kim K, et al. Synaptopodin protects against proteinuria by disrupting Cdc 42:IRSp53: Mena signaling complexes in kidney podocytes. *Am J Pathol.* 2007;171(2):415-427.
34. Wei C, Moller CC, Altintas MM, et al. Modification of kidney barrier function by the urokinase receptor. *Nat Med.* 2008;14(1):55-63.
35. Coughlan MT, Patel SK, Jerums G, et al. Advanced glycation urinary protein-bound biomarkers and severity of diabetic nephropathy in man. *Am J Nephrol.* 2011;34(4):347-355.
36. Coughlan MT, Forbes JM. Temporal increases in urinary carboxymethyllysine correlate with albuminuria development in diabetes. *Am J Nephrol.* 2011;34(1):9-17.
37. Tan AL, Sourris KC, Harcourt BE, et al. Disparate effects on renal and oxidative parameters following RAGE deletion, AGE accumulation inhibition, or dietary AGE control in experimental diabetic nephropathy. *Am J Physiol Renal Physiol.* 2010;298(3):F763-F770.
38. Toyoda M, Najafian B, Kim Y, Caramori ML, Mauer M. Podocyte detachment and reduced glomerular capillary endothelial fenestration in human type 1 diabetic nephropathy. *Diabetes.* 2007;56(8):2155-2160.
39. Weil EJ, Lemley KV, Mason CC, et al. Podocyte detachment and reduced glomerular capillary endothelial fenestration promote kidney disease in type 2 diabetic nephropathy. *Kidney Int.* 2012;82(9):1010-1017.
40. Pagtalunan ME, Miller PL, Jumping-Eagle S, et al. Podocyte loss and progressive glomerular injury in type II diabetes. *J Clin Investig.* 1997;99(2):342-348.
41. Ruster C, Bondeva T, Franke S, Forster M, Wolf G. Advanced glycation end-products induce cell cycle arrest and hypertrophy in podocytes. *Nephrol Dial Transplant.* 2008;23(7):2179-2191.
42. Chuang P, Yu Q, Fang W, Uribaldi J, He J. Advanced glycation end-products induce podocyte apoptosis by activation of the FOXO4 transcription factor. *Kidney Int.* 2007;72(8):965-976.
43. Harcourt BE, Sourris KC, Coughlan MT, et al. Targeted reduction of advanced glycation improves renal function in obesity. *Kidney Int.* 2011;80(2):190-198.
44. Zhuang A, Yap FY, Bruce C, et al. Increased liver AGEs induce hepatic injury mediated through an OST48 pathway. *Sci Rep.* 2017;7(1):12292.
45. He CJ, Zheng F, Stitt A, Striker L, Hattori M, Vlassara H. Differential expression of renal AGE-receptor genes in NOD mice: possible role in nonobese diabetic renal disease. *Kidney Int.* 2000;58(5):1931-1940.
46. Perkins BA, Ficociello LH, Ostrander BE, et al. Microalbuminuria and the risk for early progressive renal function decline in type 1 diabetes. *J Am Soc Nephrol.* 2007;18(4):1353-1361.
47. Krolewski AS, Niewczas MA, Skupien J, et al. Early progressive renal decline precedes the onset of microalbuminuria and its progression to macroalbuminuria. *Diabetes Care.* 2014;37(1):226-234.
48. Russo LM, Sandoval RM, Campos SB, Molitoris BA, Comper WD, Brown D. Impaired tubular uptake explains albuminuria in early diabetic nephropathy. *J Am Soc Nephrol.* 2009;20(3):489-494.
49. Asgeirsson D, Venturoli D, Fries E, Rippe B, Rippe C. Glomerular sieving of three neutral polysaccharides, polyethylene oxide and bikunin in rat. Effects of molecular size and conformation. *Acta Physiologica.* 2007;191(3):237-246.
50. Normand G, Lemoine S, Villien M, et al. AGE content of a protein load is responsible for renal performances: a Pilot Study. *Diabetes Care.* 2018;41(6):1292-1294.
51. Sourris KC, Morley AL, Koitka A, et al. Receptor for AGEs (RAGE) blockade may exert its renoprotective effects in patients with diabetic nephropathy via induction of the angiotensin II type 2 (AT2) receptor. *Diabetologia.* 2010;53(11):2442-2451.
52. Mallipattu SK, Uribaldi J. Advanced glycation end product accumulation: a new enemy to target in chronic kidney disease? *Curr Opin Nephrol Hypertens.* 2014;23(6):547-554.
53. Vavra JJ, Deboer C, Dietz A, Hanka LJ, Sokolski WT. Streptozotocin, a new antibacterial antibiotic. *Antibiot Annu.* 1959;7:230-235.
54. Schreiber A, Shulhevich Y, Geraci S, et al. Transcutaneous measurement of renal function in conscious mice. *Am J Physiol Renal Physiol.* 2012;303(5):F783-788.
55. Tan NY, Bailey UM, Jamaluddin MF, Mahmud SH, Raman SC, Schulz BL. Sequence-based protein stabilization in the absence of glycosylation. *Nat Commun.* 2014;5:3099.
56. Bailey U-M, Jamaluddin MF, Schulz BL. Analysis of congenital disorder of glycosylation-id in a yeast model system shows diverse site-specific under-glycosylation of glycoproteins. *J Proteome Res.* 2012;11(11):5376-5383.
57. Xu Y, Bailey U-M, Schulz BL. Automated measurement of site-specific N-glycosylation occupancy with SWATH-MS. *Proteomics.* 2015;15(13):2177-2186.
58. da Huang W, Sherman BT, Lempicki RA. Systematic and integrative analysis of large gene lists using DAVID bioinformatics resources. *Nat Protoc.* 2009;4(1):44-57.
59. Schindelin J, Arganda-Carreras I, Frise E, et al. Fiji: an open-source platform for biological-image analysis. *Nat Meth.* 2012;9(7):676-682.
60. Forbes JM, Thallas V, Thomas MC, et al. The breakdown of preexisting advanced glycation end products is associated with reduced renal fibrosis in experimental diabetes. *FASEB J.* 2003;17(12):1762-1764.
61. Wilke SA, Antonios JK, Bushong EA, et al. Deconstructing complexity: serial block-face electron microscopic analysis of the hippocampal mossy fiber synapse. *J Neurosci.* 2013;33(2):507-522.
62. Souza DBD, Gregório BM, Benchimol M, Nascimento FAdM. Evaluation of the glomerular filtration barrier by electron microscopy. In: Janacek M, Kral R, eds. *Modern electron microscopy in physical and life sciences*, vol. 09. Rijeka: InTech; 2016.

63. Choi M, Chang C-Y, Clough T, et al. MSstats: an R package for statistical analysis of quantitative mass spectrometry-based proteomic experiments. *Bioinformatics*. 2014;30(17):2524-2526.
64. Vizcaino Juan Antonio, Csordas Attila, del-Toro Noemi, et al. 2016 update of the PRIDE database and its related tools. *Nucleic Acids Res*. 2016;44(D1):D447-D456.

#### SUPPORTING INFORMATION

Additional supporting information may be found online in the Supporting Information section.

**How to cite this article:** Zhuang A, Yap FYT, Borg DJ, et al. The AGE receptor, OST48 drives podocyte foot process effacement and basement membrane expansion (alters structural composition). *Endocrinol Diab Metab*. 2021;4:e278.  
<https://doi.org/10.1002/edm2.278>